PHYSICAL REVIEW B, VOLUME 64, 125212

Carbon-tin defects in silicon

E. V. Lavrov
Institute of Radioengineering and Electronics of RAS, Mokhovaya 11, 103907 Moscow, Russia and ITTP, TU Dresden, Zellescher Weg 16, D-01062 Dresden, Germany

M. Fanciulli
Laboratorio MDM—INFM, Via C. Olivetti 2, I-20041 Agrate Brianza (MI), Italy

M. Kaukonen and R. Jones
School of Physics, University of Exeter, Exeter, EX4 4QL, United Kingdom

P. R. Briddon
Department of Physics, University of Newcastle upon Tyne, Newcastle upon Tyne NE1 7RU, United Kingdom

(Received 26 February 2001; published 11 September 2001)

Infrared absorption experiments and *ab initio* computer simulations are used to study tin-carbon centers in silicon. Electron irradiation of C and Sn doped Si leads to prominent absorption lines at 873.5 and 1025 cm^{-1}. These are assigned to a carbon interstitial trapped by a substitutional Sn atom. The calculated modes are in good agreement with those observed. The calculations also suggest that a close-by pair of substitutional C and Sn will be a stable but electrically inert defect. This defect may account for the experimentally observed drop in the concentration of the C_s-C_i defect after a room temperature annealing. Finally, we suggest Sn-C codoping of Si for manufacturing of radiation hard silicon.

DOI: 10.1103/PhysRevB.64.125212 PACS number(s): 78.30.Am, 66.30.Jt, 61.72.Bb, 61.72.Ji

I. INTRODUCTION

In crystalline silicon carbon is a common and important impurity.[1] Predominantly, carbon atoms occupy substitutional sites in the regular silicon lattice while interstitial carbon C_i is formed when mobile silicon interstitials, produced by electron irradiation, are trapped by substitutional carbon C_s.[2,3] At room temperature, C_i migrates through the lattice and becomes trapped at C_s, whereby a dicarbon center C_s-C_i is formed.[4–6] Once created, C_s-C_i may trap vacancies produced by further electron irradiation and transforms into another dicarbon center consisting of two carbon atoms occupying adjacent substitutional lattice sites C_s-C_s.[7,8] Carbon also forms many centers with other interstitial impurities. The most studied ones involve oxygen, phosphorus, arsenic, antimony,[1] and hydrogen.[9–12]

Tin being a group IV element is electrically neutral as a substitutional impurity in the diamond lattice. It's size suggests that it would be a trap for small atoms or vacancies and it has been suggested to be one of the most efficient vacancy traps in silicon.[13,14]

The first identified tin-related center in silicon was the tin-vacancy center, SnV found in electron irradiated tin-doped Si.[15,16] This defect has recently been investigated by combined deep level transient spectroscopy and *ab initio* modeling.[17] Remarkably, it was found that the defect possesses five charge states ranging from a double donor to a double acceptor. Very recent EPR studies of electron irradiated tin-doped silicon have revealed the formation of a tin-divacancy center SnV-V. Moreover, diffusion of SnV-V at temperatures above 500 K leads to formation of a di-tin-divacancy center SnV-VSn, through the reaction $(SnV-V)+Sn \rightarrow (SnV-VSn)$.[18,19]

In this work we report results of an infrared absorption study of electron irradiated silicon doped with both carbon and tin. We identify a new defect arising from the trapping of interstitial carbon by substitutional tin, C_i-Sn_s. The local modes of the defect are in good agreement with those found by theoretical modeling. Furthermore, the theoretical studies point to a substitutional carbon–tin pair as being a stable and electrically inert defect which may be one of the annealing products of C_i-Sn_s.

In Secs. II and III, details of the experimental and theoretical methods used are given. Section IV reports the experimental results found using infrared absorption measurements. Section V describes the theoretical results, and finally, our conclusions are given in Sec. VI.

II. EXPERIMENTAL SETUP

The sample used in this study Si:C:Sn was float-zone *n*-type silicon doped predominantly with carbon and tin enriched to 85% ^{119}Sn. The sample had the dimensions $10 \times 10 \times 3$ mm^3 and it was mechanically polished on the two opposite 10×10 mm^2 surfaces to ensure maximum transmission of infrared light. The concentrations of carbon and oxygen were estimated from the intensities (at 10 K) of the local vibrational mode of substitutional carbon at 607 cm^{-1} and of interstitial oxygen at 1136 cm^{-1} (see Ref. 20). The concentration of tin was determined from secondary ions mass spectroscopy. The crystal contained 4×10^{17} cm^{-3} ^{12}C, 1×10^{16} cm^{-3} ^{16}O, and 1×10^{18} cm^{-3} Sn. The resistivity of the crystal was 0.15 Ω cm, corresponding to phosphorus concentration of 5×10^{16} cm^{-3}.

The sample was irradiated with 2 MeV electrons supplied by a 5 MeV Escher Holland van de Graaff accelerator. The electrons were mass analyzed by a magnet which deflected

 ©2001 The American Physical Society

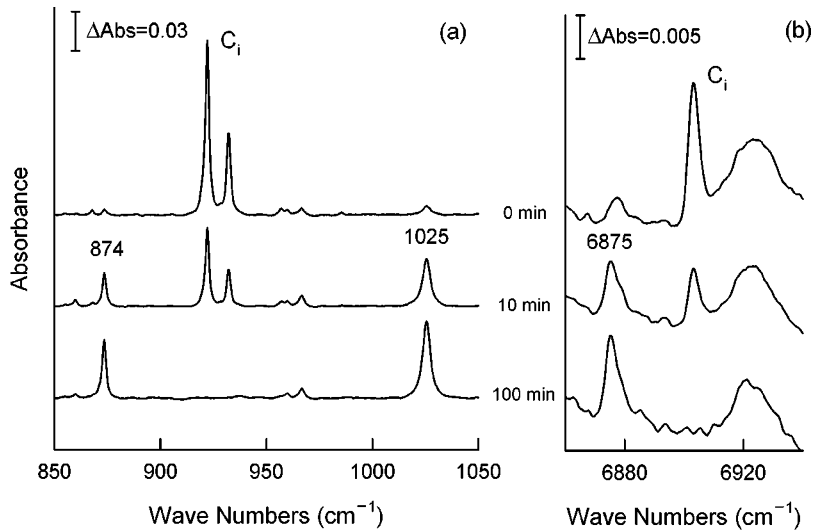

FIG. 1. Sections of absorbance spectra of electron irradiated (5×10^{17} cm^{-2}) Si:C:Sn recorded at 10 K: just after electron irradiation at 200 K, after 10 and 100 mins of room temperature annealings.

the beam into a 6 m long beamline, forming an angle of $\sim 15°$ with the exit beam from the accelerator. During the irradiation, the sample was mounted inside a vacuum chamber on a copper block, which was in good thermal contact with the cold finger of a closed-cycle helium cryocooler. The irradiation temperature was around 200 K. The irradiation dose was 5×10^{17} cm^{-2}, and the current density was kept below 2×10^{13} cm^{-2} s^{-1} to ensure that the temperature on the block did not exceed the specified value. The background pressure in the vacuum chamber was below 10^{-4} Torr.

After the irradiation, the sample was stored in liquid nitrogen before it was mounted in a closed-cycle helium cryostat designed for optical measurements. During the mounting process, the sample was allowed to warm up to room temperature for as short a time as possible (less than 10 min). This procedure was employed to reduce the diffusion of interstitial carbon created by the irradiation.

The infrared absorbance spectra were recorded with a Nicolet, System 800, Fourier-transform spectrometer. The measurements were carried out with a Ge-on-KBr beam splitter, a globar or a tungsten lamp as a light source, and a mercury cadmium telluride (MCT) detector. The spectra were recorded at 10 K with an apodizied resolution of 1 cm^{-1}.

III. THEORETICAL METHOD

The structures, electronic activity and reaction energies of carbon-tin centers in Si have been investigated theoretically using density functional theory within the local density approximation as implemented in the AIMPRO code.[21] Previously, the method has been used to investigate Sn_n-V_m defects.[17,22] The core electrons are described by Bachelet-Hamann-Schlüter pseudopotentials.[23] The valence electrons included in the calculations are $2s$ and $2p$ for carbon, $3s$ and $3p$ for silicon, and $5s$ and $5p$ for tin. Their wave functions are expressed using atom and bond centered Gaussian orbitals. The total energies of various defect geometries are evaluated in supercells along with the vibrational frequencies of the defects. These have been obtained using the harmonic approximation from the energy second derivatives between up to ten atoms closest to the core of the defect.[24] The error in the local modes found in this way is around 10%.

The electronic levels are estimated using the ionization energies and electron affinities of hydrogen terminated clusters. The calculated ionization energy of the defect in question is compared with the calculated ionization energy of a standard defect. The absolute position of the level is then obtained from the experimental level of the standard defect and the difference in the ionization energies of the defect and the standard as described previously.[25] The error in the electrical levels is around 0.2 eV. The standard defect used in this study is the carbon interstitial C_i. The experimental donor and acceptor levels of this defect are $E_v+0.28$ eV and $E_c-0.1$ eV, respectively.[5] The possible existence of second donor and acceptor levels for the carbon defects was investigated using Pt and AuH as markers.[26–28]

The supercell contains about 64 Si atoms and a $2\times2\times2$ Monkhorst-Pack mesh is used to sample the first Brillouin-zone.[29] The clusters in the electronic level calculations contain $\sim$300 atom, including the surface terminating hydrogen atoms. All the calculations are performed at 0 K.

IV. EXPERIMENTAL RESULTS

Figure 1 shows the absorbance spectra of n-type Si:C:Sn irradiated with 2 MeV electrons, as described in Sec. II, just after irradiation (top spectra) and after a room temperature annealing for 10 and 100 min. All the spectra have been referenced to Si with low carbon, tin, and phosphorus content. Intense lines at 922 and 932 cm^{-1}, seen in Fig. 1(a), represent local modes of C_i, which is formed during the electron irradiation when mobile silicon self-interstitials are trapped by C_s[1]. C_i also possesses an electronic transition at 6903 cm^{-1}, seen in Fig. 1(b), which corresponds to an excited state where an electron is weakly bound to $(C_i$-$Sn_s)^+$. The reverse process, i.e., the recombination leading to $(C_i$-$Sn_s)^0$, gives rise to the 856-meV line observed in photoluminescence.[30] C_i becomes mobile at room temperature and is readily trapped by other centers. This leads to the decrease of the C_i signals as a function of the annealing time

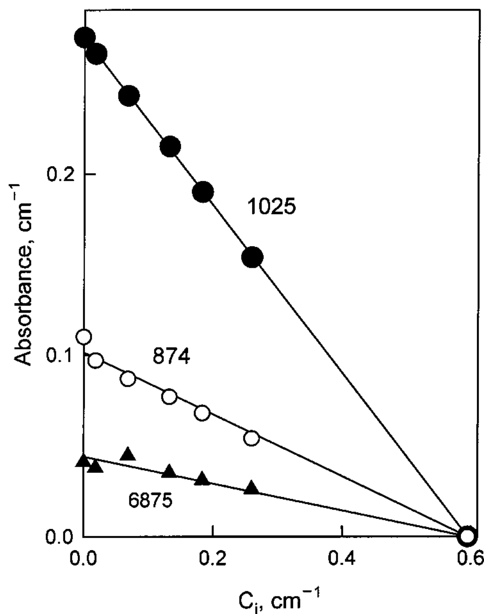

FIG. 2. Integrated absorbance of the 873.5-, 1025-, and 6875-cm^{-1} lines as a function of the integrated C_i signal measured on the 922- and 932-cm^{-1} lines.

and, as seen in Fig. 1, after 100 min of room temperature annealing C_i can no longer be detected.

Residual carbon is usually the main trap for mobile C_i in float zone silicon. The capture of C_i by C_s leads to formation of the dicarbon center C_s-C_i.[1] However, in our Si:C:Sn sample, we could not detect the parallel growth of the C_s-C_i signals,[1,6] during the annealing of C_i. Instead, new lines at 873.5, 1025, and 6875 cm^{-1} grow in the spectra, as seen in Figs. 1(a),1(b). The 873.5- and 1025-cm^{-1} lines are located in a region characteristic of the local vibrational modes of C_i, whereas the position of the 6875-cm^{-1} line suggests an electronic transition, which is also very close to the electronic transition of C_i at 6903 cm^{-1}. Figure 2 shows the integrated intensities of the three new lines plotted against the integrated intensities of the local modes of C_i. It is obvious from the figure that the lines at 873.5, 1025, and 6875 cm^{-1} have the same relative intensities and are anticorrelated with the C_i signal. This strongly indicates that they belong to the same center. This center is not stable and, after storing the sample at room temperature for several days, the new lines can no longer be detected. Only at this stage local modes of C_s-C_i appear in the spectra. Based on this, as well as on the closeness of the new modes with those of C_i, we suggest that the center responsible for the 873.5-, 1025-, and 6875-cm^{-1} lines represents a carbon interstitial perturbed by another center. This suggestion is also supported by the annealing kinetics of C_i. Measurements conducted on electron irradiated *n*-type silicon doped only with carbon in the same concentration as in our Si:C:Sn sample showed that in presence of tin, C_i anneals out 3.5 times faster.

We believe that of all possible candidates, the center is most likely a C_i defect that has been trapped by Sn. Sn is the most abundant impurity in the sample with a concentration of 1×10^{18} cm^{-3}. Another possibility, phosphorus can be

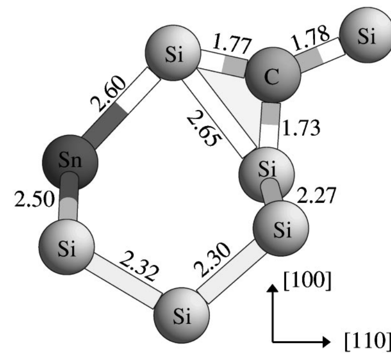

FIG. 3. Ground state configuration of the C_i-Sn_s center. The tin atom is at the next nearest neighbor position from both atoms of the C_i. Bond lengths are in [Å].

excluded by the following arguments. The concentration of C_i is estimated to be 4×10^{16} cm^{-3} from the intensities of its local vibrational modes.[1] This is about 80 % of the concentration of P but only 10 and 4 % of the concentrations of C_s and Sn, respectively. Thus C_i is most likely to be trapped by Sn. Furthermore, EPR studies of the C_i–P center find it to be stable at room temperature,[31] whereas the center responsible for the 873.5, 1025, and 6875 cm^{-1} lines anneals out at room temperature within a few days.

Another tin-related center known to be present in the as-irradiated sample is SnV. However, at most about 4% of the Sn can be tied up in this defect as the vacancy concentration cannot exceed that of C_i. Thus the dominant defect in the sample remains substitutional Sn.

The final concentration of C_s-C_i after room temperature annealing, as determined by the intensities of the local modes of the center, is approximately half of that of C_i in the as-irradiated sample. This implies that a considerable part of C_i is trapped by other centers. The lack of any additional high frequency vibrational modes would rule out another interstitial carbon species. Therefore, it is possible that a substitutional dimer pair C_s-Sn_s having modes masked by those of C_s is formed. Such a center could be formed directly by the reaction of C_i with Sn-V.

V. THEORETICAL RESULTS

We find the lowest energy of the tin interstitial–carbon defect to be one where the Sn atom lies at the second nearest neighbor position from the interstitial carbon atom. We denote this defect by $(C_i\text{-}Sn_s)^{2N}$ (Fig. 3) and define its energy to be zero. Switching the carbon atom with the undercoordinated Si atom in Fig. 3 and relaxing, leads to a less stable center with an energy of 0.25 eV. Placing Sn at a neighboring site to C_i gives to two configurations $(C_i\text{-}Sn_s)^{1N}$ which have energies between 0.5–0.8 eV higher, while the energy of a Sn atom at a third neighbor position to C_i is 0.3 eV higher than $(C_i\text{-}Sn_s)^{2N}$. Thus the most stable defect is one where the Sn atom perturbs the carbon interstitial.

The symmetry of the stable defect $(C_i\text{-}Sn_s)^{2N}$ is C_{1h} with both Sn and C_i lying in the same (110) plane. This second nearest configuration is favored because the carbon atom pulls in its two neighbors lying in the mirror plane, slightly

dilating the Si-Si bond in this plane. These are then preferential sites for the Sn atom. The Sn-Si bond has length 2.6 Å, slightly longer than 2.5 Å found for the corresponding Si-Si bond in C_i. This compressive strain compensates the tensile strain surrounding the carbon atom. The bond lengths of C_i are, however, virtually unchanged by the presence of Sn.

The calculated frequencies of the local vibrational modes of $(C_i\text{-}Sn_s)^{2N}$ lie at 905 cm^{-1} and 1036 cm^{-1} and are within 40 cm^{-1} of the measured values at 873.5 cm^{-1} and 1025 cm^{-1}. The carbon atom in the 873.5 cm^{-1} mode (symmetry A') moves in the (110) mirror plane, while it moves out of this plane in the 1036 cm^{-1} mode (symmetry A''). The calculated modes drop to 878 and 1003 cm^{-1} in the case of the ^{13}C isotope.

The isolated C_i defect introduces two Kohn-Sham levels into the band gap. The lower is filled and arises from the p orbital on carbon and leads to the donor activity of the center. The upper level is empty and is localized around the p^* orbital on the undercoordinated Si atom neighboring carbon. This leads to the acceptor level at $E_c-0.1$ eV. The presence of Sn at the second nearest neighbor position modifies only slightly the donor level arising from C_i. This follows as the energy of the p orbital on carbon lying normal to the mirror plane is virtually unchanged as its overlap with the Sn atom is negligible. The calculations demonstrate that the donor level of $(C_i\text{-}Sn_s)^{2N}$ is the same as that of C_i. Thus the donor level is placed at $E_v+0.28$ eV.

The electronic absorption at 6875 cm^{-1} in C_i is probably due to the transition of an electron from the donor level to a level near the conduction band edge. In the final state, the electron is weakly bound to $(C_i\text{-}Sn_s)^+$. This is because its transition is very close to the donor bound exciton in C_i at 6903 cm^{-1}.

Nevertheless, the dipole transition from the donor level to the unoccupied silicon p orbital is actually symmetry allowed for $(C_i\text{-}Sn_s)^{2N}$ with C_{1h} symmetry but not for the C_i defect whose symmetry is C_{2v}. Presumably, the transition matrix element for this internal transition is small as it has not been detected. Nevertheless, the unoccupied p orbital of the undercoordinated Si atom is much more affected through the presence of Sn. It now overlaps the Sn atom and is sensitive to the movement of the C and Si atoms caused by Sn. This results in the $(-/0)$ level dropping from $E_c-0.10$ eV in C_i to $E_c-0.35$ eV in $(C_i\text{-}Sn_s)^{2N}$. There are no second donor or acceptor levels.

We now discuss reaction energies for the carbon-tin defects. The reaction $C_i+Sn_s\rightarrow(C_i\text{-}Sn_s)^{2N}$ is exothermic with a binding energy between C_i and Sn of 0.35 eV. Its small value implies that the defect easily dissociates just above room temperature — as is indeed observed. Consider for example thermal equilibrium between the constituents of the above reaction. If $[C_i]=4\times10^{16}$ cm^{-3}, $[Sn]=1\times10^{18}$ cm^{-3}, then the fraction of C_i bound to Sn drops from 94% around 300 K to 34% at 400 K.

However, other reactions can be considered. A preexisting vacancy can be trapped by the defect forming $C_s\text{-}Sn_s$. The binding energy between neutral V and , neutral $(C_i\text{-}Sn_s)^{2N}$ is 5.6 eV. The product of the reaction is a substitutional $C_s\text{-}Sn_s$ pair. The lowest energy configuration of $C_s\text{-}Sn_s$ is where substitutional carbon and tin sit next at neighboring sites (see Fig. 4). The second and third nearest neighbor locations are ≈0.2 eV higher in energy than the nearest neighbor one. The $C_s\text{-}Sn_s$ defect is electrically inactive. If vacancies are released from other defects, they would be trapped by $C_i\text{-}Sn_s$ forming inert substitutional pairs. This defect may be one of the products of the anneal of $C_i\text{-}Sn_s$, however, its low binding energy implies that the defect will be *thermodynamically* unstable just above room temperature.

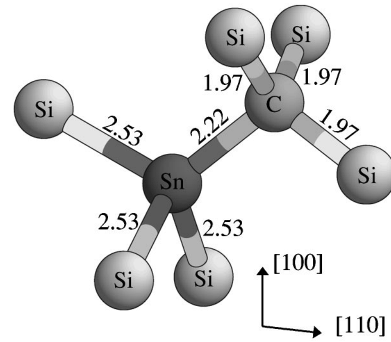

FIG. 4. The lowest energy structure for the $C_s\text{-}Sn_s$ center in which a tin atom is located next to carbon. Both atoms are near the substitutional sites. Bond lengths are in [Å].

Metastable forms of C_i-SnV defects also exist. Figure 5 shows the complex C_i-SnV where SnV has C_i as a neighbor. This defect is less stable than $C_s\text{-}Sn_s$ by 5.4 eV. The atoms in this complex are also fourfold coordinated, and it is electrically inactive. The defect possesses vibrational modes at 572 and 729 cm^{-1}, and as these are far away from 873.5 and 1025 cm^{-1}, we can exclude it being the defect observed in the irradiated material. The low frequency carbon vibrational modes arise from the very long C-Si bonds, ~2 Å present in the complex (see Fig. 5).

It has been suggested previously that carbon and tin doped Si would be a radiation hard material.[13] We suppose that interstitial and vacancies generated by radiation are preferentially trapped by carbon and tin centers, respectively,

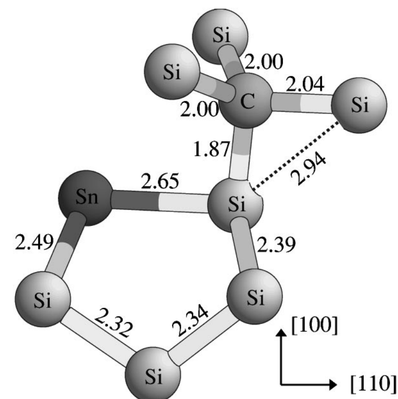

FIG. 5. Metastable C_i-SnV center. All the atoms are fourfold coordinated. The center is metastable with respect to the substitutional dimer $C_s\text{-}Sn_s$. A vacancy has been created by removing the undercoordinated Si atom in $C_i\text{-}Sn_s$. Bond lengths are in [Å].

forming mobile C_i and immobile SnV defects at room temperature. Then a subsequent recombination reaction is $C_i + \mathrm{SnV} \rightarrow C_s\text{-}Sn_s$ leading to the production of electrically inactive defects. Now, although the binding energy of C_s with Sn is very small, the diffusion energies of these atoms are very large. Thus once created, the C_s-Sn_s pair will remain frozen in the lattice.

VI. CONCLUSIONS

Electron irradiated *n*-type silicon doped with carbon and tin has been studied by infrared absorption spectroscopy. Three new lines at 873.5, 1025, and 6875 cm^{-1} are identified to arise from a metastable center in which a substitutional tin sits at a next nearest substitutional site from a carbon interstitial. The closeness of the two local vibrational modes found in the Sn doped material to C_i (within 100 cm^{-1}) and the calculated low binding energy of $C_i$with Sn (0.35 eV) — consistent with the low thermal stability of the defect — support this identification. Additionally, theoretical modeling studies demonstrate that the defect is composed of a carbon interstitial trapped by the substitutional tin center. The calculated modes at 905 and 1036 cm^{-1} are within 40 cm^{-1} of the observed modes. The donor level at $E_v + 0.28$ eV is almost the same as for the carbon interstitial and accounts for the closeness of the electronic absorption at 6875 cm^{-1} with the 6903 cm^{-1} absorption due to C_i. The acceptor level of C_i-Sn_s is calculated to lie at $E_c - 0.35$ eV and is shifted from the $E_c - 0.1$ eV acceptor level of C_i. The substitutional pair C_s-Sn_s defect is bound by 0.2 eV. It may account for experimentally observed drop in the concentration of the C_s-C_i defect after the room temperature annealing and, once formed, is likely to dissociate only at high temperatures.

Finally we believe that the reaction pathway $C_i + Sn_s \rightarrow (C_i\text{-}Sn_s)^{2N}$ followed by the reaction $(C_i\text{-}Sn_s)^{2N} + V \rightarrow C_s\text{-}Sn_s$ with overall energy gain of the order of 6 eV suggests that Sn and C codoped silicon might be appropriate material for radiation hard devices operating near room temperature.

ACKNOWLEDGMENTS

We thank J. R. Byberg, University of Århus, for numerous and fruitful discussions. This work was supported by the Danish National Research Foundation through the Aarhus Center for Atomic Physics. E.V.L. also acknowledges Alexander von Humboldt Foundation for financial support and a grant from the Russian Foundation for Basic Research (Grant No. 99-02-16652). R.J. and M.K. thank the ENDEASD network for support.

[1] For a recent review see G. Davies and R. C. Newman, in *Handbook on Semiconductors*, edited by T. S. Moss (Elsevier Science, Amsterdam, 1994), Vol. 3b, p. 1557, and references therein.

[2] A. R. Bean and R. Newman, Solid State Commun. **8**, 175 (1970).

[3] G. D. Watkins and K. L. Brower, Phys. Rev. Lett. **36**, 1329 (1976).

[4] G. D. Watkins, in *Radiation Effects in Semiconductors*, edited by M. Hulin (Dunod, Paris, 1965).

[5] L. W. Song, X. D. Zhan, B. W. Benson, and G. D. Watkins, Phys. Rev. B **42**, 5765 (1990).

[6] E. V. Lavrov, L. Hoffmann, and B. Bech Nielsen, Phys. Rev. B **60**, 8081 (1999).

[7] J. R. Byberg, B. Bech Nielsen, M. Fanciulli, S. K. Estreicher, and P. A. Fedders, Phys. Rev. B **61**, 12 939 (2000).

[8] E. V. Lavrov, B. Bech Nielsen, J. R. Byberg, B. Hourahine, R. Jones, S. Öberg, and P. R. Briddon, Phys. Rev. B **62**, 158 (2000).

[9] A. Endrös, Phys. Rev. Lett. **63**, 70 (1989).

[10] A. N. Safonov, E. C. Lightowlers, G. Davies, P. Leary, R. Jones, and S. Öberg, Phys. Rev. Lett. **77**, 4812 (1996).

[11] L. Hoffmann, E. V. Lavrov, B. Bech Nielsen, B. Hourahine, R. Jones, S. Öberg, and P. R. Briddon, Phys. Rev. B **61**, 16 659 (2000).

[12] E. V. Lavrov, L. Hoffmann, B. Bech Nielsen, B. Hourahine, R. Jones, S. Öberg, and P. R. Briddon, Phys. Rev. B **62**, 12 859 (2000).

[13] A. Brelot, IEEE Trans. Nucl. Sci. **19**, 220 (1972).

[14] A. Brelot, in *Radiation Damage and Defects in Semiconductors*, edited by J.E. Whitehouse Conference Series No. 16 (Institute of Physics, London and Bristol, 1973), p. 191.

[15] G. D. Watkins, Phys. Rev. B **12**, 4383 (1975).

[16] G. D. Watkins, Solid State Commun. **17**, 1205 (1975).

[17] A. Nylandstet Larsen, J. J. Goubet, P. Mejholm, J. Sherman Christensen, M. Fanciulli, H. P. Gunnlaugsson, G. Weyer, J. Wulf Petersen, A. Resende, M. Kaukonen, R. Jones, S. Oberg, P. R. Briddon, B. G. Svensson, J. L. Lindstrom, and S. Dannefaer, Phys. Rev. B **62**, 4535 (2000).

[18] M. Fanciulli and J. R. Byberg, Physica B **273–274**, 524 (1999).

[19] M. Fanciulli and J. R. Byberg, Phys. Rev. B **61**, 2657 (2000).

[20] *Annual Book of ASTM Standards* (ASTM, Philadelphia, 1988), Vol. 10.05.

[21] R. O. Jones and O. Gunnarson, Rev. Mod. Phys. **61**, 689 (1989).

[22] M. Kaukonen, R. Jones, S. Oberg, and P. R. Briddon (unpublished).

[23] G. B. Bachelet, D. R. Hamann, and M. Schlüter, Phys. Rev. B **26**, 4199 (1982).

[24] S. R. Elliott, in *The Physics and Chemistry of Solids* (Wiley, London, 1998), Chap. 4, pp. 218–232.

[25] A. Resende, R. Jones, S. Öberg, and P. R. Briddon, Phys. Rev. Lett. **82**, 2111 (1999).

[26] H. Zimmermann and H. Rysse, Appl. Phys. Lett. **58**, 499 (1991).

[27] E. Ö. Sveinbjörnsson and O. Engström, Appl. Phys. Lett. **61**, 2323 (1992).

[28] E. Ö. Sveinbjörnsson, G. I. Andersson, and O. Engström, Phys. Rev. B **49**, 7801 (1994).

[29] H. J. Monkhorst and J. D. Pack, Phys. Rev. B **13**, 5188 (1976).

[30] J. Thonke and J. Weber, Solid State Commun. **61**, 241 (1987).

[31] X. D. Zhan and G. D. Watkins, Phys. Rev. B **47**, 6363 (1993), and references therein.